APPLICATION OF SIMILARITY PRINCIPLES AND TURBULENCE RESEARCH TO BED-LOAD MOVEMENT

by

Dr. Ing. A. Shields

Translated from:

"Anwendung der Aehnlichkeitsmechanik und der Turbulenzforschung auf die Geschiebebewegung," Mitteilungen der Preussischen Versuchsanstalt fur Wasserbau nd Schiffbau,

Berlin, 1936

by W. P. Ott and J. C. van Uchelen

HYDRODYNAMICS LABORATORY
CALIFORNIA INSTITUTE OF TECHNOLOGY
PASADENA
PUBLICATION NO. 167

Soil Conservation Service
Cooperative Laboratory
California Institute of Technology
Pasadena, California

United States Department of Agriculture
Soil Conservation Service
Cooperative Laboratory
California Institute of Technology
Pasadena, California

APPLICATION OF SIMILARITY PRINCIPLES AND TURBULENCE RESEARCH TO BED-LOAD MOVEMENT

by

Dr. Ing. A. Shields

Translated from:
"Anwendung der Aehnlichkeitsmechanik und der Turbulenzforschung auf die Geschiebebewegung," Mitteilungen der Preussischen Versuchsanstalt fur Wasserbau und Schiffbau, Berlin, 1936
by W. P. Ott and J. C. van Uchelen

CONTENTS

APPLICATION OF SIMILARITY PRINCIPLES AND TURBULENCE RESEARCH TO BED-LOAD MOVEMENT

by

Dr. Ing. A. Shields

Translated from:

"Anwendung der Aehnlichkeitsmechanik und der Turbulenzforschung auf die Geschiebebewegung," Mitteilungen der Preussischen Versuchsanstalt fur Wasserbau and Schiffbau, Berline, 1936 by W. P. Ott and J. C. van Uchelen.

Introduction

The principal difficulties in solving a problem concerning bed-load movement in a river are: 1) inadequate knowledge of the natural processes, and 2) the unavoidable lack of similarity in model experiments.

In order to gain general information regarding bed-load movement, one is in the first place dependent upon experiments in model flumes, wherefrom laws can be deduced, which - under certain conditions - are applicable to bed-load movement in rivers. However, they will not cover all bed-load problems encountered in hydraulic engineering. Moreover, the unavoidable dissimilarity between model and river must be limited as far as possible in order that the results may be transferable with some measure of accuracy.

The following experiments were made in the Prussian Experimental Institute for Hydraulic and Ship Construction in Berlin, with the objective of determining the influence of the weight and shape of grains upon the movement of water and bed load.

This treatise consists of four parts. In the first section a method is given for computing the effective force of flowing water upon a subdivision of the perimeter and upon the corresponding water volume (assuming the perimeter of the cross-section to be equally rough at all points. In this instance, the formulae derived herefrom are applied to a rectangular channel, and provide simple expressions for essential magnitudes.

With an uneven roughness of the perimeter these magnitudes were best graphically determined with the aid of the velocity distribution in the channel center.

The second section considers primarily the conditions at the beginning of bed-load movement. By treating the acting forces statistically, and utilizing the experimental results of rough pipes, the tractive-force coefficient $\frac{\tau_o}{(\gamma_1 - \gamma)d}$ could be determined as a function of the

expression $\frac{v_* d}{\nu} = \frac{d}{\delta}$. The dependence of this function upon the grain shape is described in detail.

The third section deals with bed-load movement from three different angles; first, constancy of a certain manner of movement is investigated, as this constitutes the required basis for all further computations. Secondly, the various manners of movements are classified and described. In the third place, the methods of compiling empirical formulae are discussed.

The fourth section describes the experimental bed-load materials, apparatus, and method of procedure.

Section 1. Transferability of Experimental Results.

The strongest objection against mutual comparability of the results of model experiments - obtained from a channel with a rectangular, cross-section - and against the transfer of these results to full-scale conditions, lies probably in the absence of a similarity of shape. Different water depths, in a uniform channel breadth, represent different cross-sections. Were it possible, the results of experiments in channels with a variable, finite breadth ought to be transferred to a channel of infinite breadth, as this would not only provide a common basis for comparison, but in most cases would also closely approach the conditions found in natural rivers. The attempt to use the so-called hydraulic radius $R = A/P$ (also called perimetrical depth - i.e., cross-sectional area A divided by the wetted perimeter P) discloses the fact that this is an arbitrary method, because the hydraulic radius does not take sufficient account of the shape of the channel. This magnitude is derived from investigations in closed pipes of uniform boundary roughness; by measuring the resistance under elementary conditions, good results were obtained. The question arises whether this magnitude is applicable to an open channel. It is necessary therefore to consider the open channel fundamentally in the following manner: First of all, the momentum principle is to be applied to the total cross section, the boundary areas to be drawn as shown in Fig. 1. Summarizing the change in momentum (Impulskräfte) over areas 1 and 2, one finds:

$$\rho \int_0^{D_1} \int_0^{B_1} v_1 v_1 \, dDdB = \rho \int_0^{D_2} \int_0^{B_2} v_2 v_2 \, dDdB = 0$$

and the pressure force to be:

$$\int_0^{D_1}\int_0^{B_1} p_1 dDdB - \int_0^{D_2}\int_0^{B_2} p_2 dDdB = 0$$

in uniform flow there will exist only the friction forces and pressure forces resulting from the weight of the water. Consequently, the component of the weight in the direction of flow must be equated to the total shear upon the perimeter:

$$\gamma BD \sin\alpha = B\tau_{\text{bottom}} + 2D\tau_{\text{wall}} + B\tau_{\text{air}}$$

with small α, $\sin\alpha \sim \tan\alpha = S$ = slope.

Disregarding the friction of air, and writing:

$$B\tau_{\text{bottom}} + 2D\tau_{\text{wall}} = (B + 2D)\tau_{\text{mean}}$$

it follows that:

$$\gamma BDS = (B + 2D)\tau_m \text{ and } \tau_m = \gamma S \frac{DB}{B+2D} = \gamma S R_m$$

In this way, therefore, the application of the hydraulic radius merely yields a shearing stress, as averaged over the wetted perimeter. As a rule, this shearing stress should not be equated to the tractive force (Schleppspannung).

In order to determine the particular force at the bottom, the principle of momentum must be applied to the bottom as follows:

Boundaries of area subdivisions are drawn through the corners of the bottom and perpendicular to the isovels of the stream. Fig. 2 shows the subdivisional areas.

Since the dividing areas cut the isovels perpendicular, there are no shearing forces transferred along these areas.[a]

---

a See also: Leighly-University of California Publications in Engineering, 1934. (The temporally occurring shearing stresses, due to turbulent variations, are equalized.)

Again disregarding air resistance, a summation of the forces in the flow direction - with the introduction of sin α = s - results in:

$$\gamma A_b S = B \tau_{bottom} \qquad \text{thus} \quad \tau_b = \gamma S \frac{A_b}{B}$$

and

$$\gamma A_w S = 2D \tau_{wall} \qquad \text{thus} \quad \tau_w = \gamma S \frac{A_w}{2D}$$

What remains to be determined are the subdivisional areas A_b and A_w.

Investigation of a series of isovels shows that in composite cross-sections, with perimeters of uniform or irregular roughness, where $\frac{v_* d}{\nu} < \sim 0.05$ (see Page 16 and J. Nikuradse[1] page 10) a desired approximate division of the cross-section can be attained by means of middle and angular division lines.[b]

---

b This would only be valid for the primary flow. However, since the secondary flow occurs along middle and angular dividing lines (see Prandtl), the distribution of the cross-section would not be affected. The secondary flow, therefore, causes only a modification of the distribution of shear over a perimetrical area, without changing the total shear over this area. In an open channel this picture is partly distorted, owing to air friction and surface tension of the water. Nevertheless, measurements show that the above supposition here also is justified.

According to this method, we find for the bed of a rectangular, open channel:

$$\tau_b = \gamma SD\left(1 - \frac{D}{B}\right) \qquad \text{for } 0 \leq \frac{D}{B} \leq \frac{1}{2}$$

and

$$\tau_b = \gamma S \frac{B}{4} \qquad \text{for } \frac{D}{B} \geq \frac{1}{2}$$

while for the walls

$$\tau_w = \gamma S \frac{D}{B} \qquad \text{for } 0 \leq \frac{D}{B} \leq \frac{1}{2}$$

and

$$\tau_w = \gamma S \frac{B}{2}\left(1 - \frac{B}{4D}\right) \qquad \text{for } \frac{D}{B} \geq \frac{1}{2}$$

If the subdivisions of the perimeter are designated by P_1, P_2, P_3, P_4, ... P_n and the corresponding subdivisions of the cross-section by A_1, A_2, ..., A_n then the ratios A_1/P_1, A_2/P_2 ... $A_n/P_n = R_1$, R_2 ..., R_n are subdivisional hydraulic radii, as distinguished from the total hydraulic radius $R_m = A/P$.

It is easily realized that, for an open rectangular channel $R_b = R_w = R_m$ (respective: $\tau_b = \tau_w = \tau_m$) is only valid if $D/B = 1/2$, and, further, that $R_b = R_m$, or $\tau_b = \tau_m$ for infinite breadth, and $R_w = R_m$, or $\tau_m = \tau_w$ for infinite depth. In other respects they differ (see Fig. 3).

In the expressions thus far obtained, only force was considered. But one must also know, for instance, the volume of water to be attributed to the bed - that is, the magnitudes of the mean velocities for the subdivisional areas.

In case the subdivisional radii are all of equal magnitude and the perimeter is of the same roughness throughout the cross-section, the mean subdivisional velocities would be identical, or $v_1 = v_2 \ldots = v_n \ldots = v_m$. According to our calculation - that is, in case the subdivisional radii are, as usual, dissimilar - v_n is indicated by the following formula:

$$v_n = \sqrt{2gS} \sqrt{\frac{R_n}{\lambda_n}} = C\sqrt{R_n S}$$

Here R_n is considered as known on account of the foregoing computation. λ_n, as a rule, is not invariable, even though the conditions of the perimeter are identical, and must be computed according to the well known resistance formulae of Karman[3], Nikuradse-Prandtl[4], Nikuradse[1]. For re-examination one may refer to the equation:

$$Q = v_m A = \Sigma v_n P R_n$$

where Q represents the measured rate of discharge and v_n the computed subdivisional velocities. These computations are rather tedious. Moreover, since it is still a question whether or not application of the results of circular-conduit experiments is permissible for the subdivisional cross sections in question, it is advisable to express the mean part-velocities in relation to the mean cross-sectional velocity. Since:

$$\sqrt{2gS} = \frac{v_n}{\sqrt{\frac{R_n}{\lambda_n}}} = \frac{v_n}{\sqrt{\frac{R_m}{\lambda_n}}}$$

it follows that:

$$v_n = \left(\frac{\lambda_m}{\lambda_n}\right)^{1/2} v_m \left(\frac{R_n}{R_m}\right)^{1/2}$$

Only the relation λ_m / λ_n is here to be considered as unknown. However, since in practice R_n is not very different from R_m, and the dependence of λ upon R is relatively slight, the assumption $\lambda_m / \lambda_n = 1$ - provided the subdivisions of the perimeter represent similar conditions - will involve inappreciable error. Thus, the mean subdivisional velocity becomes:

$$v_n = \left(\frac{R_n}{R_m}\right)^{1/2} v_m \qquad (2)$$

and consequently the discharge will be:

$$v_n A_n = v_n P_n R_n = P_n R_n \left(\frac{R_n}{R_m}\right)^{1/2} v_m$$

Measurements of velocity in cross-sections with walls of uniform quality definitely confirm this relation.

It would be enlightening to check the above development by experimentation. Two pertinent experiments are known: one by Engels[5], who measured the intensity of shear at the bottom of a rectangular open channel, and, later on one by Schober[6], who for the same measurements utilized moveable plates of similar roughness on bottom and walls. Engels' measurements proved insufficient for checking the above equations. Schober's measurements were carried out with $D/B = 0.3$. R_b therefore differed appreciably from R_m. These experiments are thus suitable for such a check. The relative values obtained by Schober may be expediently used, in the form of the ratio of wall and bottom shear. According to previous concepts $\tau_w / \tau_b = 1$ (since R_m is used in place of R_b). According to the computation of the hydraulic radii of the cross-section subdivisions:

$$\frac{D}{B} = 0.3 \qquad \frac{R_w}{R_b} = \frac{\tau_w}{\tau_b} = 0.715$$

After the work of Schober with

$$\frac{D}{B} = 0.3 \text{ and } \frac{C_b}{C_w} = 1$$

Velocity of Water	τ_w / τ_b	
m/sec	theoretically	after measurements of Schober
0.1	0.715	0.66
0.2	"	0.732
0.3	"	0.685
0.4	"	0.711
0.5	"	0.710
0.6	"	0.722
		mean 0.703

The above table represents a compilation of Schober's values τ_w / τ_b for various velocities of the water. The tabulated values of τ_w / τ_b represent mean values of all of Schober's measurements, and are sufficiently confirmative to warrant the introduction of a hydraulic radius for the subdivisions - particularly at high velocities, when errors in measurements are comparatively small.

The statement regarding the mean velocities of the subdivisions embidied in the formula

$$v_n = \left(\frac{R_n}{R_m}\right)^{1/2} v_m$$

is also supported by the isovel patterns of Nikuradse and others. Nevertheless, such computations are more or less inaccurate on account of the fact that the boundary dividing lines, which stand perpendicular to the isovels, cannot be determined precisely.

In case the perimeters are of different roughness, and $v_* d/\nu > \sim 0.05$, the cross-sectional distribution is governed not only by the profile form (partly also by air-friction, surface tension and secondary flow) but likewise by dissimilarity in the roughness of the walls. This "relative roughness" becomes more decisive, the more the relative roughness of one perimetrical subdivision differs from that of another. Knowledge of this relation is still too inadequate to permit establishing ordinary equations which would take into consideration the form of the cross-section subdivision and the effect of the

"relative roughness", as well as other factors. However, to reach a general conclusion, it is necessary that the quantity of discharge be a maximum value, the latter being an additional requisite. For a knowledge of the processes involved, velocity measurements are necessary in order to construct the isovel patterns. On the other hand, since the construction of a complete isovel pattern requires laborious work and is often unnecessary, it is more practical to determine a portion of the pattern. Measurements in an open channel were carried out in the following manner:

A Pitot tube was placed upon a bridge in such a manner that the tube could be moved horizontally across in the channel. A perpendicular velocity distribution in the middle zone was next recorded. In order to determine to what width the velocities of the middle zone extended, the Pitot tube was then gradually moved across the channel. In this manner the region of validity for this velocity distribution was quickly established.

Thereupon tractive force and mean velocity were graphically determined, this region also being decisive for bed-load movement.

The value of the tractive force in this region was determined by the level of the maximum velocity. As long as this maximum velocity was maintained at the surface, it was possible to use the water depth in this computation. Up to the time the bed was excessively developed, re-examination of the tractive force was possible, since no influence was exercised by the walls, and the turbulence could develop freely. Thus,

$$\frac{u}{v_*} = a + b \log \frac{v_* d}{\nu} + 5.75 \log \frac{y}{d} = A + 5.75 \log \frac{y}{d} . \qquad (3)$$

with quadratic resistance.[c]

c See pages 10 and 5. The k in the Nikuradse's designation is replaced by d, which is more customary in Hydraulics.

Since, by plotting u over log y, a straight line results with an inclination of 5.75 v_*, one has:

$$\tau = \frac{\gamma}{g} v_*^2 = \frac{\gamma}{g} \left(\frac{\text{Incl}}{5.75} \right)^2$$

This formula proved to be comparatively accurate for appreciable depths.

At lesser depths it was not as satisfactory, due to inadequate determination of the inclinations. However, the maximum velocities have always appeared at the surface, so that the water depths were decisive. Moreover, where the straight line cuts the y = l axis at u = u_l one has, for quadratic resistance:

$$\tau = \frac{\gamma}{g}\left(\frac{U_l}{A + 5.75 \log \frac{l}{d}}\right)^2$$

Since Nikuradse's value A = 8.48 is valid only for a definite roughness (see Influence of Grain Shape), A - provided τ is known - could be computed. This resulted in A - values which are approximately 4.0% smaller.[d]

---

d In one plotting of $\frac{u}{v_*}$ against log $\frac{y}{d}$ the gradual roughening of the bed, due to its development, could be determined by systematic deviations. The magnitude of A for the various kinds of roughness with a quadratic resistance is then given by equation (3) and

$$\frac{283}{\sqrt{\lambda}} - 5.75 \log \frac{R}{d} + 3.75 = A$$

A is a characteristic hydraulic parameter for a given roughness, and determines, together with the relative roughness the magnitude of λ (and hence of C).

Figs. 4 and 5 illustrate the plotting of u against y in logarithmic form for various water depths with constant slope. It is obvious that the friction of air and the surface tension induce a somewhat premature rounding-off of the curves in the proximity of the surface.

Concluding Remarks to the First Section

In this section it has been shown how the shear and discharge can be computed for part of a perimeter - for instance, for the bottom. The practical value of those computations lies in the fact that the experimental results are no longer dependent upon model forms (i.e., the experimental channels). Thus, they can be transferred directly to nature. The methods here used also give an insight into the effect of changes in form (for instance, in the case of depth distortion in a model). An isovel pattern clearly shows that a particular tractive force at the bottom of a model may be influenced, to a large extent, by including part of the cross-section of the walls. Moreover, the effect of planned alterations in the cross-section of rivers can be foreseen.

2. Beginning of Bed-Load Movement.

The preceding chapter illustrated how the total tangential force of water at the bottom can be computed by means of the isovels and may be approximated with the aid of the above equations. Proceeding with the problem of the beginning of bed-load movement, it is necessary to consider the force which is exerted upon the grains of the uppermost layer of the bed, and to keep in mind that only the grains of this layer are being moved. This force does not necessarily have to correspond to the total shear since the grains somewhat below the bed surface also absorb part of the shearing force of the water. (Of course these lower grains indirectly also take up the shearing force of the upper grains). In the following discussion this is taken into account by proceeding from the equilibrium of the grains on the bed-surface (or, approximately, the uppermost layer).

Moreover, only the functional relation between such equilibrium and measurable flow magnitudes is being sought, and not theoretical values (as, for instance, sphere resistance after Prandtl, Oseen and others). Further, it is realized from the start that the question of bed-load movement is a matter of statistics, and must be treated as such. Grain properties, in formulae, can only be laid down in a statistical sense.

Owing to turbulence, the velocity of the water must be characterized by its mean values[e] (later it will be seen that this turbulent motion is essential).

e To measure the momentary velocities special measuring instruments would be required. However, this is of no concern here.

Considering the grains in a bed of uniform grain sizes, the question is: When will the grain be dislodged from the bed and set into motion? How the grain moves will not be investigated here. Moreover, it is assumed that the movement is small. The state in which the grains start moving will later be designated as "the beginning of movement", and is experimentally to be determined by extrapolating the bed-load transport curve to the time bed-load movement ceases.[f]

f To this end the flow conditions in the proximity of the bed-load trap have been particularly observed, in order to include the very small quantities of bed load at the beginning of the movement. On the other hand, the bed was levelled carefully, in order to avoid movement of projecting grains ahead of the real initial movement. The more uniform the grain group and the smoother the bed, the more accurately the beginning of movement may be determined. In case of mixed bed load, the beginning of movement cannot definitely be

established in this manner, because of the possible removal of only a part of the grain-sizes (for instance, the finer ones). In that case, one must refer to a certain and partly arbitrary determination of this boundary. (See Kramer, 7, and Casey, 8). The so-called "weak" movement, after Kramer and Casey, corresponds most closely to the beginning of movement.

Consequently, it is only a question of force with which we are confronted - namely, how great (statistically) is the resistance of the grain to movement? And, how great is the force exerted by the flow upon the upper grain layer?

First the resistance of a grain (that is, the force required to dislodge a grain from a bed of uniform grain size) is to be considered. In other words, the force required to move a grain on a bed of uniform grain-size. This force is known to be proportional to the weight of the grain; thus:

$$K_0 = \alpha_2(\gamma_1 - \gamma)\alpha_1 d^3$$

where

γ_1 = specific weight of the grain

γ = specific weight of the fluid

d = mean grain diameter

α_1 = porosity of the uniform bed load, dependent only upon the grain shape, and density of deposition.

α_2 = friction coefficient. It represents the relation between grain-resistance (during movement on a bed of uniform grains) and grain weight. This value is dimensionless, and depends solely upon the grain-shape and the density of deposition. (The condition of the grain surface is included in the concept "grain shape".)

The force component along the slope here is at the utmost 1% and may be neglected.

Both values α_1 and α_2 depend exclusively upon the grain shape and the deposition and may therefore be combined $\alpha_{1\,2}$. $\alpha_{1\,2}$, for grain shape, in a statistical sense, is a constant value.

From the point of dimensional considerations, the effective force of the flow upon the grain is expressed in the following manner:

$$K_0 = \zeta \alpha_3 d^2 \gamma \frac{u_c^2}{2g}$$

represents a decisive grain area (α_3 again depending solely upon the grain shape). $\gamma (u_c^2/2g)$ indicates the stagnation pressure of a critical velocity. ζ depicts the resistance-coefficient of the grain at a velocity u_c.

We will not go into any further definition of the above magnitudes, or attempt to describe the aspect of the flow about the grain. We refer rather to the work of Nikuradse (V. D. I. Forschungsheft 361) where a similar type of roughness was considered (see Influence of Grain Form), and in which the essential magnitudes were carefully measured. There, on page 8, we see that in a rough pipe the following law for velocity prevails:

$$\frac{u}{v_*} = 5.75 \log \frac{y}{d} = f\left(\log \frac{v_* d}{\nu}\right)$$

wherein:

u = local velocity

$$v_* = \sqrt{\frac{R \frac{dp}{dx}}{\frac{\gamma}{g}}} = \sqrt{g\, RS} = \text{the so-called friction velocity}$$

y = distance from the wall

d = mean grain-size of the roughness (-k in Nikuradse's designations)

ν = kinematic viscosity

We are concerned here with the velocity which is critical for the grain y being equal to cd and proportional to d and c representing a constant value of the order of magnitude 1. By introducing these values one obtains:

$$u_c = v_* \left(5.75 \log c + f\left(\log \frac{v_* d}{\nu}\right)\right) = v_* f_{\alpha_4}\left(\frac{v_* d}{\nu}\right)$$

The symbol f_{α_4} signifies that this function (and others) are likewise dependent upon the grain shape (see Influence of Grain Shape).

Generally, the resistance coefficient of the grain depends upon both the grain shape and the Reynolds' number. Thus, we write this coefficient in the form: $\zeta = f_{\alpha_5}\left(\frac{u_c d}{\nu}\right)$, where f_{α_5} expresses the grain-shape dependence.

If we insert for v_c:

$$\zeta = f\alpha_5 \frac{v_* f\alpha_4 \frac{v_* d}{\nu}}{\nu} = f\alpha_{4-5}\left(\frac{v_* d}{\nu}\right)$$

the resultant force of flow upon the grain will be:

$$\zeta \alpha_3 d^2 \gamma \frac{u_c^2}{2g} = f\alpha_{4-5}\left(\frac{v_* d}{\nu}\right) \alpha_3 d^2 \gamma \frac{\left(v_* f\alpha_4\left(\frac{v_* d}{\nu}\right)\right)^2}{2g}$$

$$= \alpha_3 d^2 \gamma RS\, f\alpha_6\left(\frac{v_* d}{\nu}\right)$$

The force of the flow exerted upon the grain at the beginning of movement becomes equal to the force required to start a grain moving; thus:

$$\alpha_2(\gamma_1 - \gamma)\alpha_1 d^3 = \alpha_2 d^2 \gamma RS\, f\alpha_6\left(\frac{v_* d}{\nu}\right)$$

or:

$$\frac{\gamma RS}{(\gamma_1 - \gamma)d} = \frac{\tau_o}{(\gamma_1 - \gamma)d} = f\alpha\left(\frac{v_* d}{\nu}\right) = f\alpha_1\left(\frac{d}{\delta}\right) \qquad (5)$$

where

τ_o = critical tractive force

$\frac{v_* d}{\nu}$ = Reynolds number of grain

$f\alpha$ = a function dependent upon grain shape

$\delta = C\frac{\nu}{v_*}$ = boundary-layer thickness [see v. Karman (9)]

$(\gamma_1 - \gamma)d$ is proportional to the tangential resistance of a layer of grains (thickness = d) per unit area.

The result can, therefore, be more simply expressed in the following manner:

The relation of the effective force of water parallel to the bed to the resistance of a layer of grain is a universal function of the

ratio of grain size to the thickness of the laminar boundary layer. Accordingly, we can plot the magnitude $\tau_o/(\gamma_1-\gamma)d$ as a function of $v_* d/\nu$ and add the grain-shape influence as a parameter. The result is the curve shown in Fig. 6, which clearly indicates that the points for a bed load of uniform grain size and angular shape yield a single curve.

The trend of this very enlightening curve is explained in a simple manner with the aid of Figs. 7 and 11 in Forschungsheft 361, page 7.[1] Four different regions must be distinguished.

In the first region the thickness of the laminar-layer is greater than the mean grain-size ($\delta > d$): consdquently, no additional energy loss is caused by the roughness as compared with the energy loss over a smooth bed; the bed is therefore equivalent to a smooth surface. Thus, a zero bed velocity will exist, yet with an intensity of shear of $\mu\frac{du}{dy}$, (μ = dynamic viscosity). The grains presumably could have been dislodged by a preponderant momentary action of this force; that is, the shearing force per grain $\mu\frac{du}{dy}d^2 = \tau d^2$ on the bed surface must lift a grain of $\alpha_1(\gamma_1-\gamma)d^3$ weight from the bed (α_1 = porosity, as previously mentioned), by turning it about its point of contact on the downstream side. Since a maximum value is sought, the side forces, which would exert a retarding effect upon this movement, are neglected, and we have:

$$\tau_o = \alpha_1(\gamma_1-\gamma)d, \quad \frac{\tau_o}{(\gamma_1-\gamma)d} = \alpha_1$$

where, for uniform, angular, sharp-edged grains, α_1 has approximately a value of 0.6. This relation in Figs. 6 and 7 results in a corresponding classification and it is easily observed that the points for the finest bed-load types still lie far away. The course of the curves of similar bed-load weights in this region will be horizontal as in Fig. 7. In Fig. 6 this trend is shown as a straight line, with an inclination of 45° and is described as smooth. These lines are obtained by extrapolation and result in a critical value.

$$\frac{\tau_o}{(\gamma_1-\gamma)d} = \frac{0.1}{\frac{v_* d}{\nu}} \quad \text{thus} \quad \tau_o = \left(\frac{\gamma}{g}\right)^{1/3}\left[0.1\nu(\gamma_1-\gamma)\right]^{2/3} \qquad (6)$$

The important fact hereby is that only the parameter of the fluid and the specific weight of the grain are expressed. The grain size is omitted. Thus the reduction of the grain size no longer affects the critical shearing stress, which now may be found by diminishing the magnitudes $\frac{\gamma}{g}$, ν, and $(\gamma_1 - \gamma)$. This region extends to $v_* d/\nu \sim 2$.

In the second region, the thickness of the laminar layer is of the same order of magnitude as the mean grain size ($\delta \sim d$). At the protruding parts eddies develop, and we observe that the shearing force of the flow is most effective in this region, since $\tau_0/(\gamma_1 - \gamma)d$ has a minimum value of

$$\frac{\tau_0}{(\gamma_1 - \gamma)d} \sim 0.03 \tag{7}$$

reached at

$$\frac{v_* d}{\nu} \sim 10.$$

In the third region, the laminar layer has become so small that the flow resistance is almost exclusively governed by eddy formation. Consequently one would expect that the shearing force of the flow would exercise a constant influence upon the upper grains so that the relation $\tau_0/(\gamma_1 - \gamma)d$ remains constant. Instead, however, it increases with increasing $v_* d/\nu$. This occurrence may be explained as follows.

Although the main flow is subject to quadratic resistance, the resistance of the grain in the bed is far from quadratic, due to the low velocity which prevails in the region of this roughness. ζ, therefore, does not lie within the region of the quadratic resistance - that is, it is not constant, but decreases with increasing Reynolds number, as in the case of the sphere or the disc. However, our development of critical tractive force, for quadratic flow resistance, would result in the following simplified expression:

$$\frac{\tau_0}{(\gamma_1 - \gamma)d} = \frac{\alpha}{\zeta} \tag{8}$$

Here we see that a decrease of ζ signifies an increase of $\tau_0/(\gamma_1 - \gamma)d$, which is in accord with experimental results.

The preceding consideration could be continued in order to anticipate a fourth region, with still greater $v_* d/\nu$ values - that is, a region in which not only the quadratic resistance of the channel flow prevails, but also the resistance of the flow about the grain. Here also ζ = a constant value, as is $\tau_o/(\gamma_1 - \gamma)d$ (= constant value). Unfortunately, no definite information in this respect is available, and an estimation of this constant value can only be obtained through very undertain extrapolation. It follows that:

$$\frac{\tau_o}{(\gamma_1 - \gamma)d} \sim 0.06 \qquad (9)$$

This region would then begin at $v_* d/\nu \sim 10^3$ and would remain as long as is constant. It is possible that ζ later on decreases still farther (similar to a sphere or disc, in which case $\tau_o/(\gamma_1 - \gamma)d$ would accordingly increase abruptly.

In connection herewith the traction experiment, with concrete tetrahedrons five and ten inches in height, by the American experimental institute (U.S.W.E.S.[10]) may be mentioned. These experiments were not made on a uniform bed (as would be required for our purpose) but at regular intervals in a smooth bed, and resulted therefore in much lower values. However, it is of importance that the ten-inch tetrahedrons needed exactly twice as much tractive stress as the five-inch - that is, that the relation $\tau_o/(\gamma_1 - \gamma)d$ is constant.

Practical application of Fig. 6 is rendered somewhat more difficult, on account of the fact that τ_o occurs in $\sqrt{(g/\gamma)}\,\tau_o d/\nu$. However, this is easily overcome in the following manner: First, one computes $(\gamma_1 - \gamma)d$ and utilizes an approximate τ_o - value derived from Fig. 7. With this τ_o one now computes $\sqrt{(g/\gamma)}\tau_o d/\nu$, deducing the exact value from Fig. 6. A repetation of the computation is in most cases unnecessary.

The trend of the curves for amber and brown coal in Fig. 7 is yielded by Fig. 6, assuming that $\nu = 0.012$ and $\gamma = 1$.

Influence of Slope

In the ultimate functional relation for the beginning of movement, the slope appears only in relation to the hydraulic radius of the cross-section

for the bed. Therefore, only the product RS is decisive for the beginning of movement, though an important exception must be mentioned - namely, in case the slope becomes very appreciable. In this case RS is no longer constant for the beginning of movement but increases with increasing slope and decreasing depth. The explanation of this occurrence lies in the fact that with decreasing depths the relative roughness d/R increases in such a manner that it no longer represents a roughness, but a change in the cross-section. This occurrence was also observed by Nikuradse; he states that the relative roughness $d/R > \sim 1/15$ leads to erroneous results. Our bed-load experiments give a somewhat lower limit; that is, the deviations are first noticeable with d/R values greater than $\sim 1/25$. To be sure, a limit of approximately 1/40 should not be exceeded. This limit, which one may consider as the "limit of relative roughness", is very important, because the results of model experiments are of no value for river construction over and above these limits.

This holds in particular for experiments with shooting flow, since all of these were made with appreciable slopes (>1:200); i.e., with too small depths.

Influence of Mixture

At this point, the very careful and detailed experiments with sand mixtures by Casey[8] in the VWS may be mentioned. Casey[g] determined that

g M = ratio of the area A_f of the sieve curve below the mean value to the area A_o above d_m, see Fig. 8.

for mixtures with the modulus M 1/3, the mean grain size diameter d_m (solely decisive for the beginning of movement) must be used. The results of experiments with mixtures of this character obtained by Kramer[7] and others (in the VWS and the USWES[11] in Vicksburg) are in close accord with Casey's findings. The small deviations may be due to the determination of the beginning of movement of a mixture, and partly also to dissimilarity of the grain shapes. It must be assumed that the limit of validity in Fig. 6 increased correspondingly. This is an important addition, because most of the sand mixtures occurring in nature fulfill this constion (M > 1/3).

Influence of Weight

Since $M > \frac{1}{3}$ is also valid for the investigated type of brown coal bed load[12], we can plot the corresponding points in Fig. 6. The obvious conformity,[h] together with the conformity of barite and granite bed load

h Here the brown coal mixture III represents an exception in that the separation and cementation of finer parts lead to a somewhat higher critical tractive stress.

furnishes evidence that the influence of weight upon the beginning of movement has been fully covered.

Influence of Grain Shape

The grain shape may influence the beginning of movement in just as many respects as the α-values appearing in derivations of the equation for the beginning of movement. They were as follows:

α_1 = influence of grain shape upon porosity

α_2 = influence of grain shape upon bed-friction coefficient

α_3 = influence of grain shape upon grain surface

$f\alpha_4$ =expresses influence of grain shape upon flow conditions in a channel

$f\alpha_{4-}$ expresses influence of grain shape upon resistance coefficient (ζ).

It is evident from Fig. 6 that these α's may exert opposing influences upon the beginning of movement. It is apparent that the points for rounded grains and sharp-edged grains lie somewhat higher than those for angular grains. It would be difficult to draw more curves to express the grain shape parametrically. In order to illustrate this point, α must be investigated separately. The porosity α_1 can be easily determined. α_1, α_2 may possibly be determined by experiment; that is, by scattering a few grains on a board with uniform grains glued on to it, then by gradually inclining the board while slightly shaking it (corresponding to turbulent fluctuations), until the grains roll off. In this manner the critical slope can be determined.

The function $f\alpha_{4-5}$ may probably be estimated by settling experiments. $f\alpha_4$ is partly clarified by means of the following experiments:

The roughness used by Nikuradse[1] consisted of uniform sands of a shape designated as "rounded" and closely corresponding to the sand types

used by Casey. Neither Nikuradse nor others have made experiments in pipes with angular grains; however, experiments in open channels with granite fragments of angular shape (type 2-3 mm with very sharp edges) were availalbe to clear up this point. To determine definitely the influence of the grain shape requires that all other variables - mechanical and hydraulic - be eliminated. Accordingly, the experiments with granite grain-types were made not only with the same uniform grain sizes (d = 0.85 mm, d = 1.23 mm, d = 2.44 mm) and in the same channel, but also with the same slopes, and by using the same experimental technique as used by Casey in his sand experiments.

The results for grain sizes 0.85 mm and 2.44 mm are very characteristic and are depicted in Figs. 9 and 10 with λ plotted against Re. The illustration shows that the λ-values for the many-edged grains lie every time about ten per cent higher than those for rounded sands - i.e., an angular grain produces a greater flow resistance than a rounded one. Thus, the mean velocity, with constant RS, is less with fragments than with sand.

These results, if brought into accord with Karman's formula, indicate that in the general equation of Nikuradse[1]

$$\frac{283}{\sqrt{\lambda}} - 5.75 \log \frac{R}{k} + 3.75 = a + b \log \frac{v_* k}{\nu} = A \qquad (10)$$

with a quadratic resistance, the constant value A ~4.0 per cent ought to be smaller than the one mentioned by him. The present experiments do not furnish more accurate quantitative values for this equation (see Hydraulic Radius). This does not influence the validity of the equation for the beginning of movement, since in this case only the form of the relation after Nikuradse was used.

Measurements of the velocity-distribution in an open channel, with angular bed load at the bottom, confirm the above conclusion.

A noteworthy corroboration of these laws is also furnished by the collected "bed-velocity measurements in natural rivers" of Schaffernak[14] who gives the following empirical formula:

$$v_{bm} = k(hS)^{0.5} = 316\, k\sqrt{\gamma DS} = (142 \text{ to } 272)\sqrt{\gamma DS}$$

(D = depth in cm, k = 0.45 - 0.86). Since the quadratic resistance law

prevailed here, the Nikuradse expression is:

$$\frac{u}{v_*} = 8.48 \log \frac{y}{d}$$

or

$$u = 8.48 \log \frac{y}{d} \cdot \frac{\sqrt{\gamma DS}}{\rho} = 8.48 \sqrt{\gamma \frac{DS}{\rho}} = 2.66 \sqrt{\gamma DS}$$

One realizes that the introduction of $y = k$, and $\rho = \frac{11}{981}$ furnishes a constant value within the limit[5] given by Schaffernak.

Both types, granite fragments and same, of Fig. 6, behave differently - according to their grain diameter. Although the two granite grain types have a greater flow resistance than the two sand grain types of similar size, the plotted point for the angular granite fragments ($d = 0.85$ mm) lies somewhat above the corresponding point for same. This can only be explained by the fact that sharp-edged granite fragments have a much higher bed-friction coefficient α_2. Experiments showed that, long before the beginning of movement, a pronounced tremble occurred which was caused by the interlocking of the sharp edges.

Amber bed load, which has sharp-edged grains, likewise shows a greater critical tractive force. Consequently, one would expect a slightly greater critical tractive force in case the bed load contains very sharp-edged particles.

Conclusion Second Section

In the whole procedure leading to equation (6), no simplifying assumptions have been made. It is shown that the coefficient of the critical tractive force $\tau/(\gamma_1 - \gamma)d$ merely becomes a function of $v_* d/\nu$ though all factors have been considered. This relation is graphically depicted in Fig. 6, showing the numerical values of this function. Thus, the problem of the beginning of movement is essentially clarified, which should prove helpful in practice. Fig. 6 gives the relations at the beginning of movement between all natural and artificial grain groups of any weight, not only for the model but also for the river (see Section 1). This knowledge of the beginning of movement constitutes the basis for further studies regarding bed-load movement.

Section 3. Transportation of Bed Load

The established equations furnish quantitative results - at least in a statistical sense - since only a smooth bed was considered; that is, a bed of relative roughness, the hydraulic characteristics of which for the most part were known. In continuing our studies of the motion following the beginning of movement, this basis is no longer available, on account of the various possibilities of bed formation.

The shape and type of bed formation is decisive for bed-load movement in two respects:

1. It determines the hydraulic conditions, in that both flow and bed formation are interdependent.

2. It determines bed-load movement, in that every type of bed formation (dunes, etc.) forms a self-contained system (beginning of movement, transportation, and deposition), the interchange of bed load with adjoining ripples, or dunes, being of negligible significance.

Thus, one must proceed from the bed formation as a starting point and solve three problems, namely:

1. One must determine the constancy of a form of movement and the time required for the attainment of this condition (for instance, from a smooth bed on).

2. The various bed formations and water surfaces must be measured and described in a dimensionless form (for instance, in relation to the water depth); that is, similar formations (the water depth is also to be considered in this approximation) must be compared and an empirical dimensionless number for the different conditions deduced.

3. The bed-load movement under the various conditions of 2 must be determined and an empirical law for the movement of bed load under these various conditions derived.

Condition of Constancy

With regard to No. 1, one must first examine whether or not there exists a condition of constancy. In some cases, this will be rather difficult to determine, particularly when long-period occurrences develop, so that the time required for such experiments lies outside practical limits. Gilbert[15] made a specific experiment, in which he showed that uniform movement of but a few grains (approximating the condition of the beginning of movement) does

not endure, due to the fact that after a certain time a bed with permanent slope and discharge is being attacked at various points. This process gradually leads to an undulation of the bed, in connection with a substantially greater bed-load movement. This has also been observed in experiments with fine sand, granite fragments, and barite, inasmuch as slight ripples, immediately after the beginning of movement, spread over the entire bed.[i]

---

i In these cases (provided uniformity exists) the movement stages of "mean" and "general" movement mentioned by Kramer[7] and Casey[8] are not to be considered.

In the experiments with coarser grains this uniform movement appeared to be constant (to some extent after more than one hour of experimenting). However, it remains a question whether or not a certain bed transformation may still take place after several hours (requiring perhaps very long periods of time for the changes).

The further stages of movement, too, are subject to this uncertainty. With long dunes, the movement gradually becomes constant. This can be determined only to a certain extent, due to the variety of dune formations within an experimental section. (For these cases the number of banks in the experimental section is given). On the other hand, in a bed formation requiring shorter periods of change - for instance, in case ripples occur - the bed formation seems less variable. Such constancy is soon reached. Thus, in general, one may say that the shorter the period required for a change in the manner of movement, the greater its constancy and the shorter the time required for reaching this condition. (In a sense, this is also valid for a uniform movement, which may be considered as being similar to an infinitely long period of change.) It is noteworthy that light bed-load particles - brown coal and in particular amber - can produce the same bed formation (that is, a similar shape of ripples, dunes, etc.) as sand, barite, etc., but with a much smaller velocity of the grains, and accordingly, with a correspondingly longer period of change. Experiments show the validity of the above statement also in this case. Furthermore, it may be added as a law for certain forms of bed development that the lighter the bed load, the longer the period of movement and the less permanent the bed formation.

Since the bed load is always supplied evenly, the channel length required, in order for the bed load to reach its ultimate form of movement, is also

partly dependent upon the constancy of this motion. Moreover, this length is likewise dependent upon the size of the bed formation (or the approximate depths of the scour holes).

The persistence of the type of motion and the time required for establishing this condition is of importance, because in many experiments with a movable bed this period indicates the pertinent time scale for bed-load movement. (See Krey[16]).

For instance, after the rate of discharge and depth of the model have been established and a sediment mixture has been chosen which will undergo bed-load movement more or less similar to that occurring in nature, the experiment must continue until a state of constancy is reached. Of course experiments with a river model with bends, etc. may require a different time scale from that of experiments with a straight channel. However, results obtained with experimental channels furnish valuable facts (barring meander formation). It should not be forgotten that in some cases the condition of constancy is probably only approached asymptotically. However, the observer will be in a position to judge the approximation to which, for all practical purposes, the experiment gives sufficiently accurate results.

Shape of Bed Formations

While it is difficult to approach similarity between two flow occurrences over a flat bed, on account of the relation existing between channel breadth and water depth and the relative roughness (grain size: water depth), the problem is made even more difficult by the numerous possibilities of bed formation. Besides the similarity requirements of a smooth bed, one finds in addition the requirements of similar bed formations.

By transferring the width of the channel to an infinite width (see Hydraulic Radius) and neglecting the influence of the relative roughness d/R because of the predominant effect of the bed shape (perhaps the relative unevenness of the bed or its undulation) an example is presented of the constancy of the geometrical similarity of two processes depicted in Fig. 11.[j]

---

j By geometrical similarity the slope in both processes must be kept identical. The maintenance of similar water-surface forms also probably requires that the Froude numbers be identical. Reynolds' principles of similarity of channel flow are of less importance, as shown in Section 2.

Thus, apart from the relative roughness, three variables are to be considered:

1. The form of the water surface
2. The water depth
3. The bed shape

At the present state of scientific investigation it is practically impossible to fulfill all three requirements and one must be satisfied with a consideration of bed shape and water depth.

It suffices to designate the bed shape merely by the relation of height to length, and of bed development irregularities of the bottom. Added unto this is the extent of bed development, which is best expressed dimensionlessly by the relation of the height of the ripples, dunes, or scour holes to the water depth. No further definitions will be attempted, for even in an experimental channel length, bed formations show noticeable variations. For the present, bed formations can therefore only be classified in general terms.

If the ratio of height to length is relatively large, these formations are called ripples. Experiments have shown that fine bed load induces the formation of ripples. The finer the bed load, the greater is this tendency. (See Kramer[7], Krey[16], and others.) The relation of the height of the ripples to the water depth may become so great that the ripples are "disturbing" (see Kramer[7]). However, since the experiments were made with small grains and a correspondingly low water depth - so that the relative grain size (grain size/water depth, etc.) was constant - the reason for this ripple formation can only be attributed to the invariable parameters γ, g, and ν.

By experimenting with bed materials of various densities, it was possible to vary the controlling effect of γ and g. This led to the observation that the viscosity ν in the term $v_* d/\nu$ is the principal factor in the formation of ripples. The ν-effect can be explained from the standpoint of the laminar boundary layer, due to the fact that movement only takes place under flow impulses which bear upon the "back" of the ripples and penetrate the laminar layer. If this is not the case, the grain movement stops abruptly, so that the movement is momentarily limited to a small area. Fig. 6 shows that ripple formation only occurs when the beginning of movement is strongly influenced by the viscosity.

The coarser the grain material, the more the ratio between height and length of bed formation decreases, while at the same time - as shown in Fig. 6 - the manner of bed-load movement changes in the following sequence: scales, short banks, long banks (frequently of oblique shape) until when the values $v_* d/\nu$ are very large, the bed shows merely a gentle undulation. The ratio between height and water depth likewise gradually decreases. Thus, the various manners of movement - at least shortly after the beginning of movement - can be roughly indicated by the number[k] $v_* d/\nu$.

---

k That is, equal Reynolds numbers for the grains are the main requisite for similar manners of movement.

Fig. 12 for instance, gives an illustration of ripple formation of fine barite, while Fig. 13 shows an oblique bank formation of brown coal. With an increase of tractive force it was generally noticed that with different manners of movement, the bed shapes became shorter and higher. This shortening of the banks is related to an increase in grain velocity, and gradually leads to an overleaping of the bank heads until the water begins to flatten the bed formation. These occurrences are plotted in Fig. 6. The classification of these various states of movement is not to be understood as being numerical, nor is this meant to be a final solution of the problem of movement, but rather should be considered as a suggestion, showing that this classification is not as hopeless as it sometimes appears to be.

This is an opportune point to describe bed-load movement in shooting flow, since this process could not be presented in Fig. 6. Shooting discharge often causes short, high (standing) waves which attack the bed correspondingly and bring about a particularly strong bed-load movement. The crest of the wave lies above the crest of the ripple. These short bed undulations are not distributed over the entire channel width, but are found only in very small, longitudinal strips of approximately one and a half meters at various points along the experimental channel. This undulation pattern is superposed upon the usual bed formation (given in Fig. 6), the oblique banks of granite fragments (2-3 mm) or the bed unevenness of barite (3-4 mm), and varies in position and shape.

Bed-Load Movement

In order to clarify by means of experiments the systematic nature of bed-load transportation, it is necessary to proceed on the basis of complete

similarity. Therefore, in order to establish a law for bed-load transportation, it is necessary, among other things, that the requirements for geometrical similarity (explained in Fig. 11 and on page 27) are also fulfilled. However, it is obvious that the observation of these laws leads to a complication of the problem. Therefore, to begin with, the simplifying suppositions mentioned on the foregoing pages must be applied; that is, the processes must mainly be judged according to the bed formations. In accordance with the aforementioned classification, an attempt must be made to write a formula for the various states of movement. Limiting ourselves, we will establish only one single equation excluding certain types of movement. However, this procedure is only justified in view of the fact that experiments dealing with this similarity problem are lacking, and is carried out with full reservation so as to arrive at a quantitative premise.

For this reason we begin by excluding from our considerations bed-load movement in the form of ripples, since this is a special form of movement which has but little practical significance in comparison with natural processes. Thus, an attempt is made to establish a formula for much smaller H/L - values (height; length of bed formation) such as occur shortly after the beginning of movement (that is, the shortening of the bed formation that gradually leads to a flattening of the bed). On the right side of this equation only one function $\tau/(\gamma_1 - \gamma)d$ appears; (namely: $\tau - \tau_o/(\gamma_1 - \gamma)d$, since at $\tau = \tau_o$ the bed-load movement must be = 0) which lends itself to comparison of similar types of bed formation. On the left side will appear a dimensionless term for bed-load movement - that is, bed-load movement in weight per unit of time, divided by discharge in weight per unit of time, times a function of dimensionless factors; the latter balances these various effects for similar states of movement, despite variation of individual conditions (grain, weight, slope, etc.). It is evident that the choice of this dimensionless bed-load parameter is not the only one possible, but this is of no importance.

An analysis of the dimensions of bed-load movement with disregard for the effects of viscosity - which in reality merely amounts to an exclusion of the ripple formation whereby use is made of only such magnitudes as are generally measured in river hydraulics, indicates the bed-load movement to be dependent upon the following dimensionless magnitudes:

$\frac{v^2}{Rg}$, $\frac{d}{R}$, $\frac{\gamma_1 - \gamma}{\gamma}$, S and shape factors and any combination of these magnitudes. This analysis provides:

$$\frac{\tau - \tau_o}{(\gamma_1 - \gamma)d}$$

It follows that:

$$\frac{G}{Q} f_1\left(\frac{v^2}{Rg}, \frac{d}{R}, \frac{\gamma_1 - \gamma}{\gamma}, S, \rho_1, \rho_2 \ldots\right) = f_2\left(\frac{\tau - \tau_o}{(\gamma_1 - \gamma)d}\right)$$

A plot of G/Q against $\tau - \tau_o/(\gamma_1 - \gamma)d$ seems to be the most useful presentation of this function, yet f_1 is essentially $\gamma_1 - \gamma / S\gamma$[1]

---

1 The absence of the Froude number in this empirical formula may be attributed to the general insignificance of the surface waves. The effect of the surface waves becomes noticeable only near the wave velocity, where $v = \sqrt{gD}$, that is, when $A = v/\sqrt{gD} \longrightarrow 1$. The appreciable variations in the results obtained with shooting flow are probably due to this fact. Special experiments would be required for the investigation of this process.

Thus the empirical equation is found:

$$\frac{G}{Q}\left(\frac{\gamma_1 - \gamma}{S\gamma}\right) = 10^{\frac{\tau - \tau_o}{(\gamma_1 - \gamma)d}} \qquad (11)$$

The function $\frac{G}{Q}\left(\frac{\gamma_1 - \gamma}{S\gamma}\right)$ over $\frac{\tau - \tau_o}{(\gamma_1 - \gamma)d}$ is plotted in Fig. 15. The scattering of the points is characteristic for bed-load movement measurements, and is mainly attributed to the constancy and periodicity of bed-load movement. The periodicity could partly be eliminated if the experiment was halted at the moment the bed formation - before the trapping of grains - was the same as when the experiment began. Equation (10) has not been written to depict a universal formula for bed-load movement (without ripple formation), from which numerical values may be safely deduced. It is rather an abbreviated form to express the influence of the various factors upon bed-load movement. These influences are best separately discussed.

Influence of $\tau - \tau_o/(\gamma_1 - \gamma)d$

This factor, which can be considered as an addition to the tractive-force coefficient, fulfills the important task of classifying the various states

of movement. Krey, in his Elbe experiments, already used this magnitude as a premise in forming an opinion concerning model proportions which should correspond to full scale conditions.

The points for barite, with very small proportions of height to length, are principally found with small $\tau - \tau_o/(\gamma_1 - \gamma)d$. With greater $\tau - \tau_o/(\gamma_1 - \gamma)d$, the region of appreciable values of H/L for sand, granite fragments - and with still greater $\tau - \tau_o/(\gamma_1 - \gamma)d$ also for brown coal is transgressed. Very high values of $\tau - \tau_o/(\gamma_1 - \gamma)d$, or large H/L, bring the amber results into consideration, which in our experiments were the only ones with abrasive effect. The abrasion took place at $\tau - \tau_o/(\gamma_1 - \gamma)d \sim 0.2$.

Influence of Weight

The grain weight appears three times in Equation 11. First, in $\tau - \tau_o/(\gamma_1 - \gamma)d$, where it exercises an important influence upon the classification; secondly, in G/Q, where bed-load movement - measured according to volume; and thirdly, in the function $(\gamma_1 - \gamma)/S\gamma$ where the results for bed-load groups of various specific weight were combined. We see therefore that G depends upon the second power of the weight in water.

Influence of Slope

Experiments with similar grain material show an increasing sediment discharge with greater slope. The slope in the denominator of the function $(\gamma_1 - \gamma)/S\gamma$ clearly expresses this influence.

Influence of Grain Shape

Essential influences of the grain shape upon the magnitude of bed-load movement (after the first stages) were not noticed.

Shooting Flow

As is well known, a flow is called "shooting" when the flow velocity is greater than the wave velocity; that is, $v > \sqrt{gD}$. Usually v represents the mean flow velocity $v_m = Q/A$. However, on account of the velocity distribution, the question arises, which velocity v may be considered decisive? A definite solution of this problem would be very difficult. For our purpose, the use of the mean velocity may be taken as sufficiently accurate.

The influence of the shooting flow upon the beginning of movement has been described in the preceding section, "Influence of the Slope".

Its influence upon bed-load movement has been partly treated in this section under "Movement Stages". It suffices here to add that the points for bed-load movement by shooting flow (as plotted in Fig. 15) all lie slightly higher, because of a somewhat different bed formation by shooting flow.

Advantages of Lighter Bed-Load Material

The characteristics of lighter bed-load material and their usefulness for model bed loads are evident from the experimental results previously mentioned.

Very advantageous for model experiments is the small critical tractive force hereby attainable, which is nearly proportional to the weight of the material under water. This indicates, for instance, that amber of the same magnitude as sand requires but about 1/20 of the critical tractive force of sand, in order to be brought into motion. This advantage needs no further emphasis.

However, as may be seen from Fig. 6, the characteristics of movement are not always so favorable, since the use of amber of 1.56 mm diameter causes a bed formation with scales, or short banks (see also Fig. 14) soon after the beginning of the movement. This characteristic generally indicates a deviation from similar processes in nature. It would increase the model resistance without restriction. Thus, one must resort to coarser amber types in order to come more to the right in Fig. 6 - that is, in order to obtain a more favorable characteristic of movement. Of course, a partial increase in the limiting tractive force cannot be avoided. Nevertheless, great advantages still remain.

For instance, if the amber grain is four times as large as the sand grain, its critical tractive force is still but 1/5 of that of sand. This, by way of example, would bring amber grain as used in our experiments into a type of motion yielding a gentle unevenness of the bed. The use of lighter bed-load materials is therefore of decided advantage for scientific experiments with river models.

Greater roughness of the bed, such as results from larger bed-load particles of amber, is often favorable, particularly in model distortions.

It is also very promising to obtain even more favorable characteristics by mixing various sizes of amber. The great moveablility of amber bed loads leads accordingly to great experimental difficulties, but these can be surmounted by the use of a special experimental technique.

It should be mentioned that greater $v_* d/\nu$ values may be obtained by diminishing the kinematic viscosity. However, there is a lack of suitable fluids having this characteristic.

Closing Remarks to Third Section

This chapter deals with the fundamentals of bed-load movement which are important from the practical point of view. The knowledge of the constancy of conditions is a necessary requisite for the validity of experimental results and for comparisons with nature, the constancy providing the time element for qualitative experiments. The description and classification of the various bed formations form the basis for the knowledge of bed-load movement. It is very important for the hydraulic engineer to know in what manner a given sand moves under certain conditions and what bed formation may result. This classification of bed formations is also a prerequisite in order to derive a law for bed-load movement. Equation 10 for bed-load movement is obtained by a partial observance of the principles of similarity and has been given in order that the engineer may have a simple formula with which to estimate bed-load movement of almost any type of sand, either in model or river.

The application is best illustrated by examples. Assume for a river the following measurements: velocity distribution in the vertical, slope, and size and specific weight bed material. First, one computes R_b, the distance between maximum velocity and bottom and can use the controls discussed on pages 9 and 10. The critical tractive force may be taken from Figs. 6 and 7. Figs. 6 and 10 indicate the bed formation and the manner of movement. The rate of bed-load movement can then be computed with equation 14.

If model experiments are to be made, a model bed load which gives the same formations is chosen with the aid of Figs. 6 and 10 (a lighter bed load being preferable) and the tractive force is determined. With reference to the conditions mentioned in Section I, it is essential that this tractive force must be produced in the model, especially in case of model distortion.

4. Types of Bed Load

The following table describes the bed-load types investigated:

Type	Specific Weight	Grain Size maximum mm	Grain Size mean diameter mm	Grain Shape	m
Amber	1.06	0.38 - 3.0	1.56	sharp edged	n
Brown Coal I	1.27	0.75 - 2.0	1.77	angular, rounded corners	
" " II	1.27	0.75 - 5.0	1.88	" " "	
" " III	1.27	2 - 5	2.53	" " "	
Granite Fragments I	2.69	2 - 3	2.44	" edges & corners	
" " II	2.71	1.02 - 1.5	1.23	" (sharp	
" " III	2.70	0.75 - 1.02	0.85	"	
Barite I	4.2	3 - 4	3.44	"	o
" II	4.19	2 - 3	2.46	"	
" III	4.2	1 - 2	1.52	"	
" IV	4.25	0.49 - 0.75	0.69	"	
" V	4.3	0.25 - 0.49	0.36	"	
" VI	4.2	2 - 5	2.76	"	

m Casey, "Ueber Geschiebebewegung"[8]
n Fragments resulting from the cutting of amber
o Material from Rock Crushers

The following grain shapes are distinguished:

Rounded - with more or less spherical grains

Flat - with grains which are considerably smaller in one direction than the other two

Angular - with partly rounded, partly sharp-edged fragments

The sieve curves in Fig. 16 supplement the above table.

All bed-loadsmaterial considered in this treatise may generally be defined as "angular" (kantig). Only the samples of amber and granite fragments of 2-3 mm are sharp-edged, while brown-coal types show somewhat rounded edges. However, they differ considerably in specific weight.

The samples consisting of granite fragments, which have approximately the weight of quartz sand, are of the same grain sizes as the rounded types of river sand (d, f, h) used by Casey[8] for investigating the influence of bed-load mixtures. These have been described for comparison under the caption, "Influence of Shape".

Experimental Apparatus

For the examination of barite particles I, II, III and brown coal I, II, and III, a rectangular wooden channel of 80 cm width was used - the same that was used by Kramer for his work on "Modellgeschiebe und Schleppkraft")[7]. For the experiments with barite the walls were made of lacquered wood; for the experiments with brown coal the walls were made equally as rough as the bottom by gluing brown-coal grains to the walls. Besides the experimental apparatus as used by Kramer, two rails were attached to the side walls in order to adjust the slope. Furthermore, a bed-load trap (in the shape of a slot) was provided in the bottom near the outlet, so as to reduce flow-disturbances to a minimum - a device which proved very satisfactory.

For the investigation of the other barite particles (IV and V) and of amber particles, a rectangular, glass channel of 40 cm width was used, which could be tilted - the same as used by Casey in his work, "Ueber Geschiebebewegung"[8]. In addition to the apparatus described by Casey, all point gages were of a particularly fine mechanism. The measuring points for intake and outlet were connected with open pots by means of tubes; the water level in these containers could be accurately read with these gages, so that the surface slope could be very closely determined.

Preparation of the Bed

Before each experiment the bed was leveled with particular care. In the wooden channel the leveling and measuring of the bed was done with the aid of a smoothing board sliding between the side rails. In the glass channel a measuring bridge was used for this purpose. Thereafter, a thin sheet of water, to which coloring matter was added, was made to run through the channel, color streaks disclosing the slightest unevenness, accordingly to be removed.

Experimental Procedure

Each bed-load type was investigated with an average of 4 different constant slopes. With each slope approximately 16 different water depths were obtained by a gradual increase of discharge. Each time a state of equilibrium was awaited.

The bed elevation was first determined through use of a glass plate resting on the bed. The water depths could then be measured by means of point-gage readings on the free surface, manometer readings, and point-gage readings on the gage-pot surfaces.

The water slope was measured in the same manner; thus it was always possible to make a satisfactory cross check. In the experiments with barite, the distribution of velocity was measured by means of a calibrated Pitot tube. Each time, bed load and a detailed measurement and description of the bed formations were recorded. (For further details concerning measurements we refer to the works of Casey and Kramer).

Summary

The present treatise deals with general problems of bed-load movement with particular reference to the influence of weight and shape. By the use of barite, granite fragments, brown coal, and amber, a great range of bed-load weight was obtained. Investigation of grain shape covered rounded, angular, and sharp-edged grains.

In order to transfer the experimental results to the standard basis of an infinite width, the concept of the hydraulic radius was taken fully into consideration. The hydraulic radius of the subdivisional bottom cross-section (corresponding to the depth at infinite width) was computed by drawing dividing planes through the corner-points of the bottom, vertical to the isovels of the flow. However, since the latter were not always available, methods of similarity had to be given. In the case of uniform boundary roughness this subdivision of the cross-section could be approximated by drawing center and corner-bisecting lines. For a rectangular channel, this led to the following result:

$$\frac{R_b}{D} = 1 - \frac{D}{B} \quad \text{for} \quad \frac{D}{B} \leq \frac{1}{2}$$

where R_b = hydraulic radius of the bottom, D = water depth, B = channel breadth.

If the boundary is of variable roughness, then the subdivision of the cross section is likewise governed by relative roughness between the different walls. It is then necessary to determine the isovels by velocity measurements.

Hydraulic radius, tractive force, and mean velocity of the divisional cross section were also determined graphically, whereby the accuracy could be controlled.

The mean shear at the bottom can be computed from the product of the hydraulic radius assigned to the bottom (R_b) and the slope (S), or $R_b S$.

However, since at first only the upper grains come into motion, the intensity of shear should only be computed for these upper grains. Generally, this shearing stress was not equal to the mean shear of the flow at the bottom, because the grains lying somewhat deeper immediately take over part of the tractive force, due to the flow in crevices and pores.

The equilibrium of the grain had to be taken as a premise in order to obtain knowledge concerning the process occurring in the upper grain layer. To this end the laws for flow in rough pipes were used as a basis, and without further assumption the following simple expression for the coefficient of the critical tractive force was found:

$$\frac{\tau_o}{(\gamma_1 - \gamma)d} = f_\alpha\left(\frac{v_* d}{\nu}\right) \tag{5}$$

where $v_* = \sqrt{R(dp/dx)/(\gamma/g)} = \sqrt{gRS}$ represents the friction velocity and $f_\alpha(v_* d/\nu)$ a function which can be graphically described. The systematic trend of the plot in Fig. 6 may be characterized in the four different regions as follows: In region I the critical tractive force exists where the particles first project through the laminar layer. This state produces a critical tractive force of

$$\tau_o = \left(\frac{\gamma}{g}\right)^{1/3} \left[0.1\,\nu(\gamma_1 - \gamma)\right]^{2/3} \tag{6}$$

In region II the laminar layer is of the same order of magnitude as the roughness elevations. In this region $\tau_o/(\gamma_1 - \gamma)d$ reaches a minimum value of ~ 0.033. In region III the quadratic resistance law of the channel flow prevails, though not yet for the flow around the particle. Thus in this region $\tau_o/(\gamma_1 - \gamma)d$ gradually increases. In region IV the quadratic resistance law for channel flow as well as for the flow around the particle, prevails, and the tractive-force coefficient in a restricted area becomes a constant value:

$$\frac{\tau_o}{(\gamma_1 - \gamma)d} \sim 0.06 \tag{9}$$

The grain weight is contained in the derivation from the general function of critical tractive force, and Fig. 6 shows that it fully considers the weight influence.

The grain shape should have been plotted as parameter in Fig. 6, but since the various effects of grain shape upon the critical tractive force offset

each other, no appreciable deviations due to grain shape can here be noted. Very sharp-edged grains seem to require a greater critical stress, owing to the dominating fact that the grains hook together.

The influence of grain shape upon flow may be easily observed, since a flat bed of "angular" particles always causes greater flow resistance than a bed of rounded particles. This finding, however, does not change the form of the flow laws but only the constant values included therein.

Bed-load movement has been considered from the viewpoint of manner of movement, since in the first place the latter greatly influences the flow of water, and secondly governs the movement of bed load. It has been further shown that the constancy of a manner of movement is of great importance, since it provides the necessary basis for formularization and in many cases furnished an essential time element for bed-load movement in models.

Moreover, it is to be emphasized that in setting up an equation for bed-load movement only similar forms of movement should be compared. The various initial movement stages (that is, the manner of movement shortly after its beginning; for instance, ripples, scales, banks, etc.) are satisfactorily classified by the number $v_* d/\nu$. Here it should be observed that ripples are only formed if the viscosity exercises an appreciable influence upon the beginning of movement. With great tractive forces one generally notices that the bed formations become somewhat shorter and deeper, until with very great tractive forces, the suspended particles commence to saltate over the bank crests. Experiments showed that the tractive-force coefficient for the beginning of movement in the form of $\tau - \tau_o/(\gamma_1 - \gamma)d$, is well suited to the classification of these various stages of movement.

If the first stage of movement shows a bed formation with a relatively small ratio of height to length (that is, with so-called bars or gentle elevations) the following equation for bed-load movement may be adopted:

$$\frac{G}{Q}\left(\frac{\gamma_1 - \gamma}{S\gamma}\right) = 10\,\frac{\tau - \tau_o}{(\gamma_1 - \gamma)d} \qquad (11)$$

where G/Q represents the weight proportion of the bed-load movement to the water discharge.

Fig. 15 shows that the results obtained with amber particles (which at the first stage of movement caused a motion in short banks) fit very well into this presentation. In this plot the results obtained with amber are to be found mainly at appreciable values and were the only ones in which abrasion of the banks occurred.

No noticeable influence of the various grain shapes upon bed-load movement could be determined after the first stages.

Investigations of bed-load movement by shooting flow show that the higher stages of movement yield somewhat greater values for bed-load movement, although a somewhat higher critical tractive force is required, as compared with the streaming condition. It should be emphasized that the equation (10) is not to be taken as a final equation for bed-load movement (even in restricted regions) but is merely meant to present a starting-point for systematic investigation of bed-load movement.

(End)

REFERENCES

1. J. Nikuradse: "Strömungsgesetze in rauhen Rohren" (Laws of Flow in rough pipes). Forschungsheft 361, VDI, Berlin, 1933.

2. L. Prandtl: "Über die ausgebildete Turbulenz" (Concerning developed Turbulence). Verhandlungen des 2. Intern. Kongresses für Techn. Mechanik, Zurich, 1926.

3. Th. v. Karman: "Mechanische Ähnlichkeit und Turbulenz" (Mechanical Similarity and Turbulence). Verhandlungen des 3. Intern. Kongresses für Techn. Mechanik, Stockholm, 1930.

4. J. Nikuradse: "Gesetzmässigkeit der turbulenten Strömung in glatten Rohren" (Systematic Nature of Turbulent Flow in Smooth Pipes). Forschungsheft 356, VDI, Berlin, 1932.

5. H. Engels: "Versuche über den Reibungswiderstand zwischen fliessendem Wasser und benetztem Umfang" (Experiments Concerning the Friction Resistance between Water and Wetted Perimeter). Zeitschrift für Bauwesen, 1912.

6. R. Schober: "Versuche über den Reibungswiderstand zwischen fliessendem Wasser und benetztem Umfang" (Experiments Concerning the Friction Resistance between Water and Wetted Perimeter). Dresden, 1916.

7. H. Kramer: "Modellgeschiebe und Schleppkraft" (Model Bed Material and Tractive Force). Mitteilung der Preuss. Versuchsanstalt für Wasserbau und Schiffbau (VWS), Berlin, Heft 9, 1932.

8. H. Casey: "Über Geschiebebewegung" (Concerning Bed-Load Movement). Mitteilung der Preuss. Versuchsanstalt für Wasserbau und Schiffbau (VWS), Berlin, Heft 19, 1935.

9. Th. v. Karman: "Über die Stabilität der Laminarströmung und die Theorie der Turbulenz" (Concerning the Stability of Laminar Flow and the Theory of Turbulence). Verhandlungen des 1. Intern. Kongresses für Techn. Mechanik, Delft, 1924.

10. "Investigation of Proposed Methods of Bank and Embankment Protection", United States Waterways Experiment Station, Vicksburg, Paper 12, 1933.

11. "Study of River-Bed Material and Their Use with Special Reference to the Mississippi System", United States Waterways Experiment Station, Vicksburg, Paper 17, 1935.

12. H. H. Wheaton: "Braunkohlenversuche" (Experiments with Brown Coal). VWS.

13. Th. v. Karman: "Some Aspects of the Turbulence Problem", Proceedings of the 4th Intern. Congress for Applied Mechanics, Cambridge, 1934.

14. F. Schaffernak: "Neue Grundlagen für die Berechnung der Geschiebeführung in Flussläufen" (New Basic Methods for the Computation of Bed-Load Movement in Rivers). Leipsig und Wien, 1914.

15. G. Gilbert: "Transport of Debris by Running Water". Prof. Paper 86, U. S. Geological Survey, Washington, 1914.

16. H. Krey; "Modellversuche für einen Fluss mit starker Geschiebeführung" (Model Experiments for a River with Heavy Bed-Load Movement). Berlin, 1935. (Revised report on previous experiments).

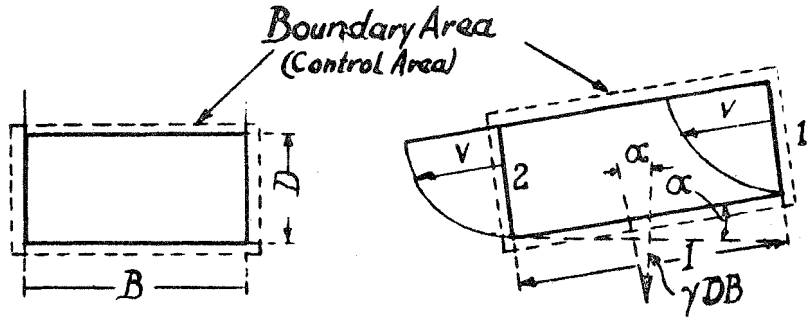

Fig. 1.

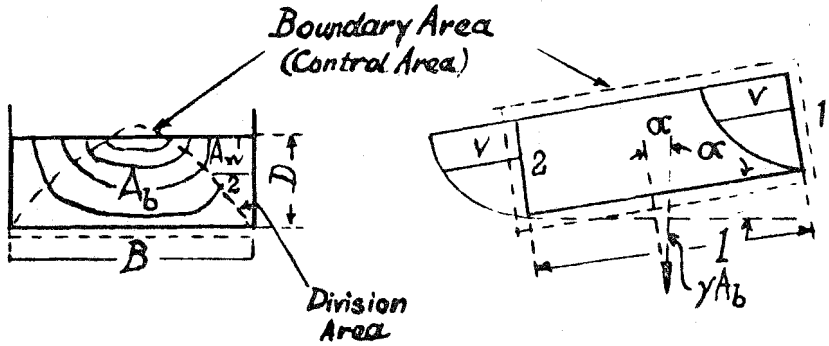

Fig. 2.

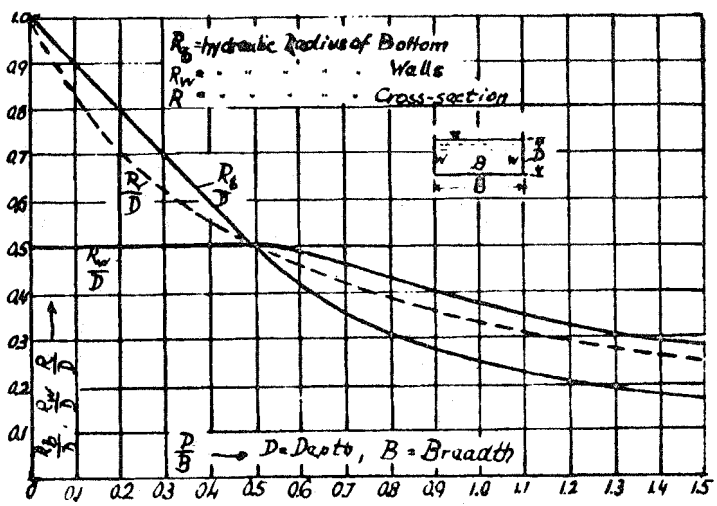

Fig. 3. Ratio of hydraulic radius to depth as function of depth-width ratio.

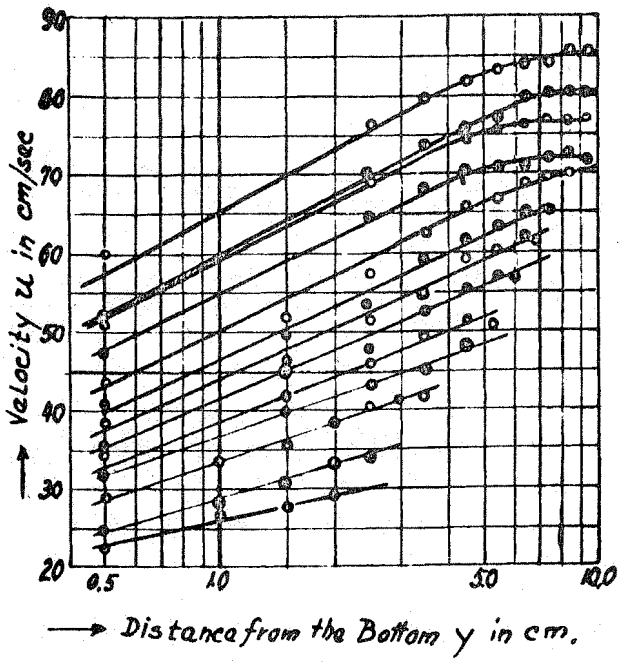

Fig. 4. Velocity distribution curves for Barite.
d = 1.52mm, S = 1/600

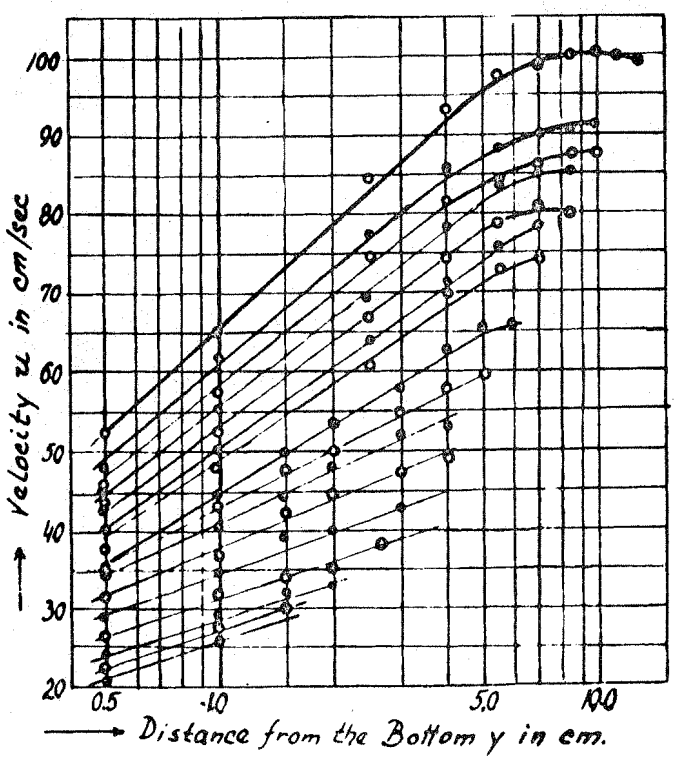

Fig. 5. Velocity distribution curves for Barite.
d = 2.46mm, S = 1/380

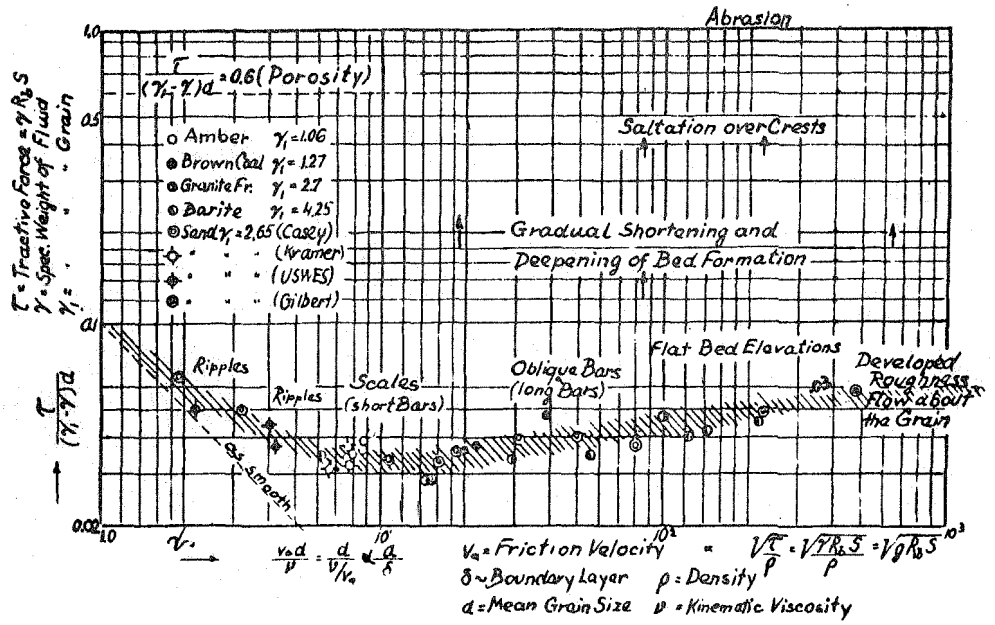

Fig. 6. Tractive - force coefficient $\frac{\tau}{(\gamma_1 - \gamma)d}$ against the Reynolds number of the grain $\frac{V_* d}{\nu}$.

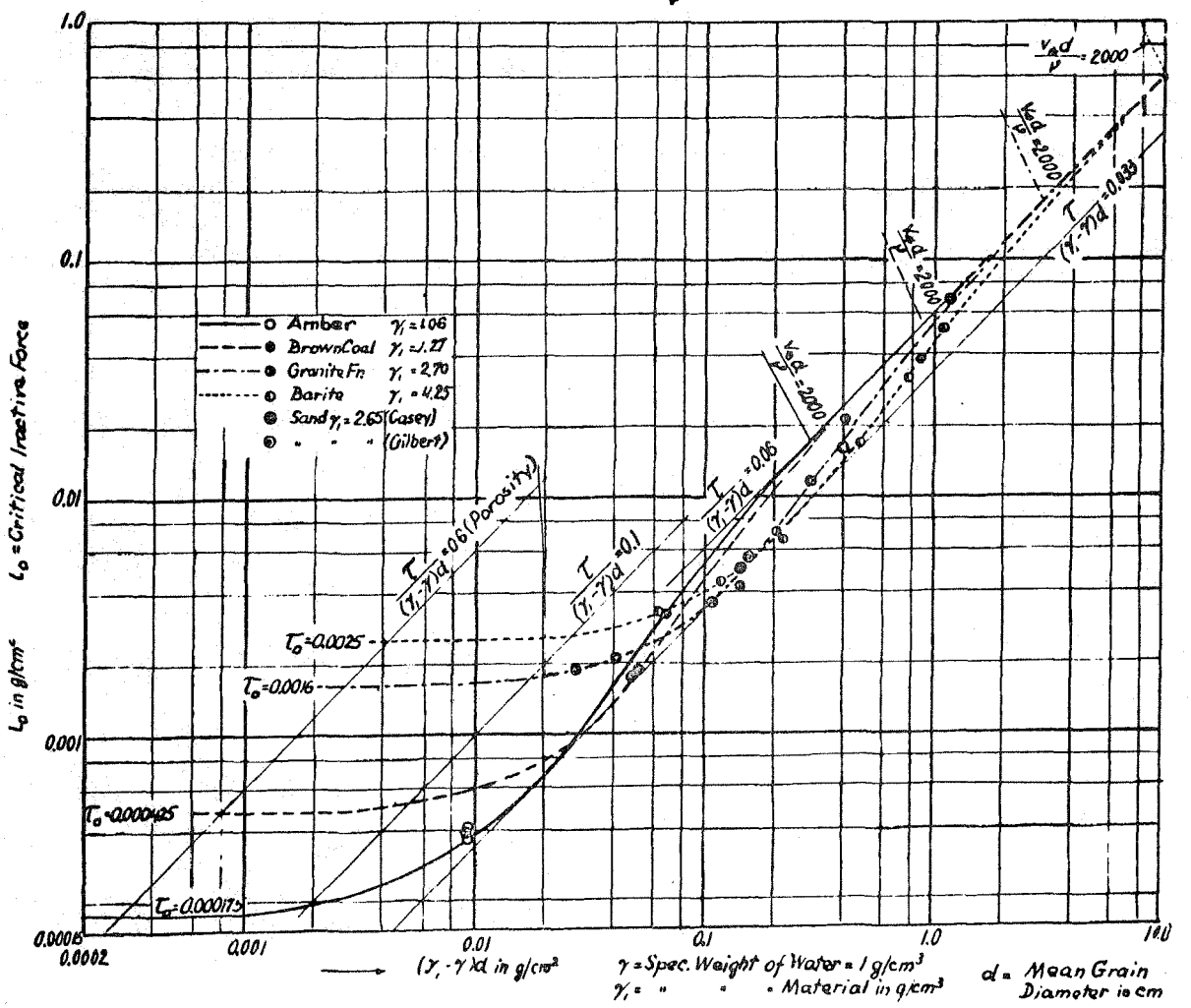

Fig. 7. Critical tractive force τ against weight of grain layers, $(\gamma_1 - \gamma)d$, (the curves are obtained from Fig. 6, assuming $\nu = 0.012$ and $\gamma = 1$).

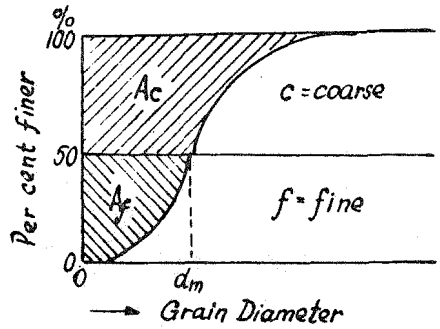

Fig. 8. Cumulative mechanical analysis curve and modulus $M = A_f / A_c$ of a bed material.

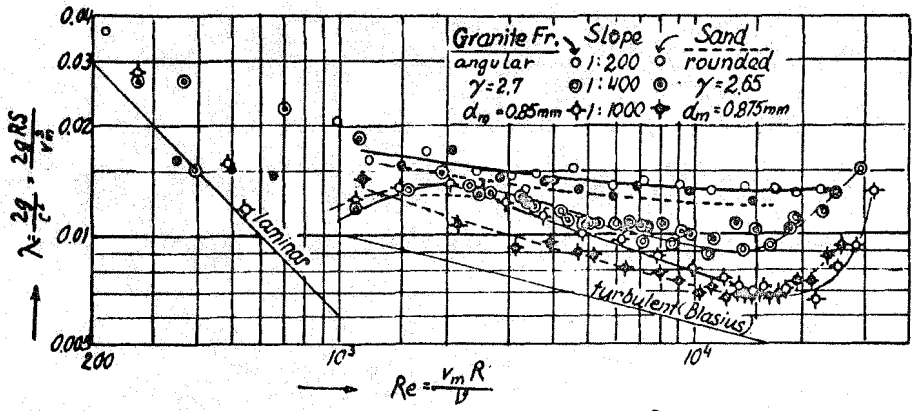

Fig. 9. Resistance coefficient λ as a function of the Reynolds number.

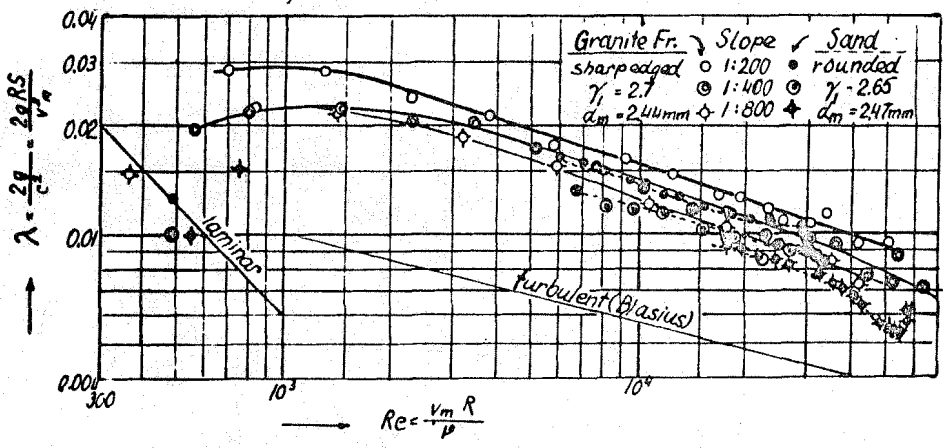

Fig. 10. Resistance coefficient λ as a function of the Reynolds number.

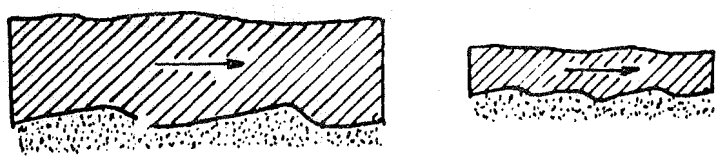

Fig. 11. Geometric similarity of two states of flow.

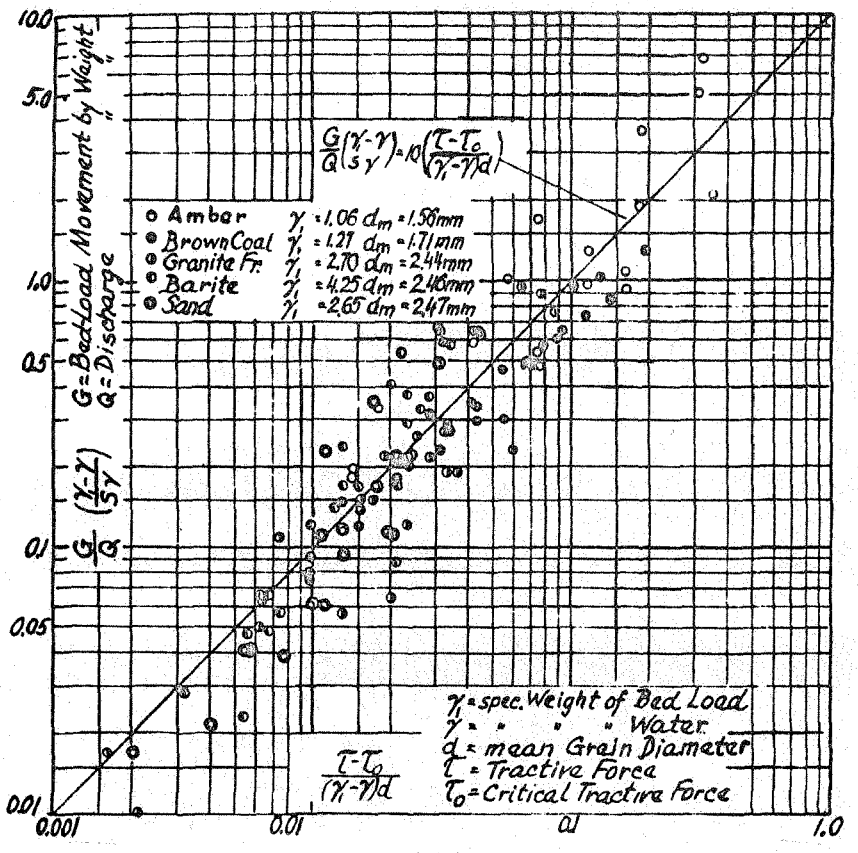

Fig. 15. Plot of empirical equation for bed-load transportation.

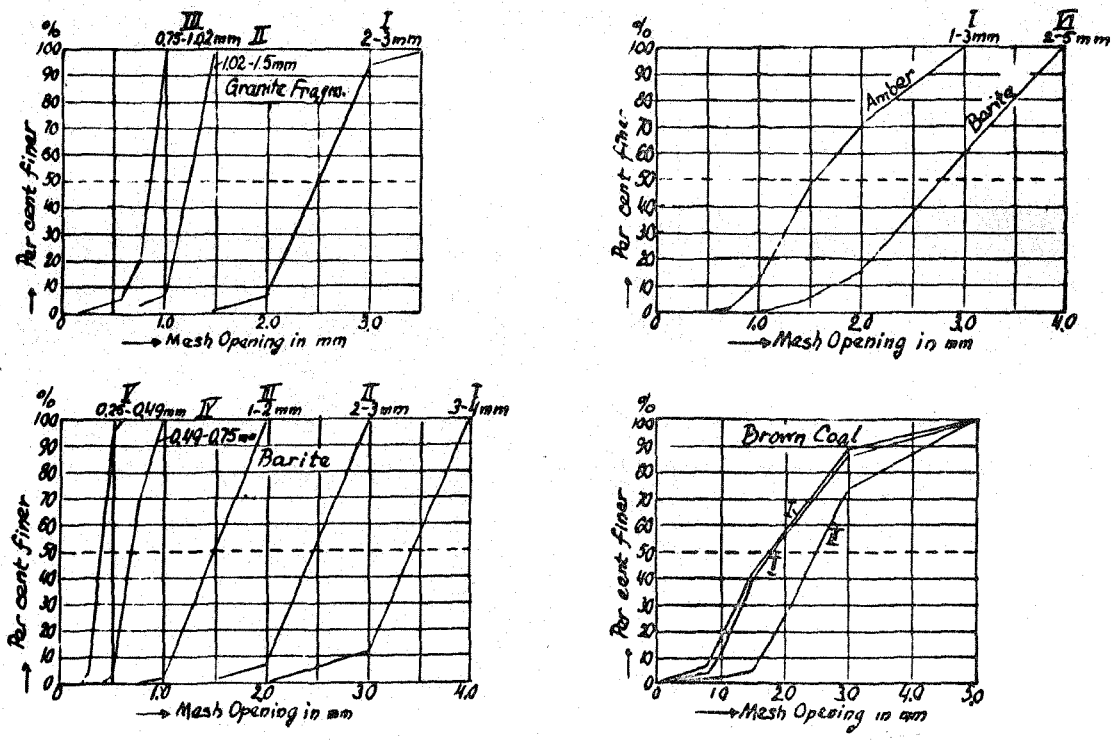

Fig. 16. Sieve analysis (square mesh).

Fig. 12. Ripple formation with baritc.

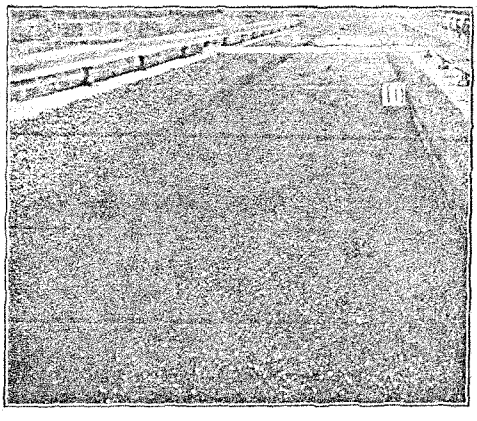

Fig. 13. Development of diagonal bars with brown coal.

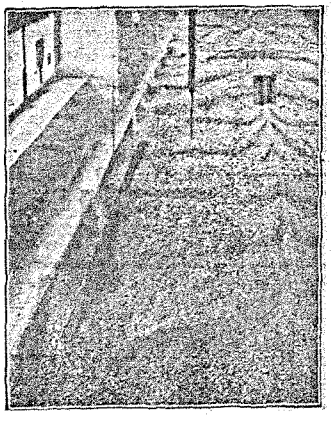

Fig. 14. "Scale" formation with amber.